

A General $T_{1\rho}$ Relaxation Model for Spin-Lock MRI using a Rotary Echo Pulse

J. Yuan¹, and Y-X. Wang¹

¹Department of Imaging and Interventional Radiology, The Chinese University of Hong Kong, Shatin, New Territories, Hong Kong

Introduction: $T_{1\rho}$ relaxation is conventionally described as a purely mono-exponential decay with respect to the spin lock (SL) time (TSL). However, B_0 and B_1 inhomogeneities can be significant sources of SL artifacts in $T_{1\rho}$ -weighted imaging and violate the validity of the mono-exponential decay [1]. As such, considerable error may be resulted by following the mono-exponential decay for $T_{1\rho}$ mapping, particularly at low SL frequencies (FSL). We present a general theoretical $T_{1\rho}$ relaxation model using a rotary echo SL pulse [2]. An analytical expression of $T_{1\rho}$ -weighted longitudinal magnetization was derived to show its dependence on off-resonant frequencies, TSL, FSL, $T_{1\rho}$ and $T_{2\rho}$ relaxation time.

Theory: A SL rotary echo pulse with FSL ω_1 was shown in Fig. 1. The magnetization evolution can be traced by using the Bloch Equation. An RF pulse is represented in the form of matrix notation $R_\phi(\Phi)$, where R denotes a rotation matrix, ϕ is the pulse orientation and Φ is the pulse flip angle ($\Phi = \omega_1 \cdot \text{TSL} / 2 = 2\pi \cdot \text{FSL} \cdot \text{TSL} / 2$). The full expression of the magnetization evolution in the presence of off-resonance $\Delta\omega_0 = 2\pi\Delta f_0$ is expressed as

$$M(t) = R_x(90^\circ) \cdot R_z(\alpha) E_\rho \cdot R_z(\alpha) E_\rho \cdot R_x(90^\circ) \cdot M(t_0) = R_x(90^\circ) \cdot R_x(-\theta) R_z(\alpha) E_\rho R_x(\theta) \cdot R_x(\theta) R_z(\alpha) E_\rho R_x(-\theta) \cdot R_x(90^\circ) \cdot M(t_0) \quad (1)$$

where $\alpha = \omega_{\text{eff}} \cdot \text{TSL} / 2$, $\theta = \tan^{-1}(\omega_1 / \Delta\omega_0)$ and $\omega_{\text{eff}} = (\omega_1^2 + \Delta\omega_0^2)^{1/2}$. E_ρ is a matrix to describe $T_{1\rho}$ and $T_{2\rho}$ relaxation as shown in Eq.2.

$$E_\rho = \begin{bmatrix} e^{-TSL/2T_{2\rho}} & 0 & 0 \\ 0 & e^{-TSL/2T_{2\rho}} & 0 \\ 0 & 0 & e^{-TSL/2T_{1\rho}} \end{bmatrix} = \begin{bmatrix} E_{2\rho} & 0 & 0 \\ 0 & E_{2\rho} & 0 \\ 0 & 0 & E_{1\rho} \end{bmatrix} \quad (2)$$

Finally, the resultant longitudinal magnetization after the SL pulse excitation can be expressed by Eq.3.

$$M_z(t) = (E_{2\rho}^2 \cos^2 \alpha \cos^2 \theta \cos 2\theta - E_{2\rho}^2 \sin^2 \alpha \cos^2 \theta + E_{1\rho} E_{2\rho} \cos \alpha \sin^2 2\theta - E_{1\rho} \sin^2 \theta \cos 2\theta) M_0 \quad (3)$$

Methods: A numerical program was developed to simulate the magnetization M_z as a function of $T_{1\rho}$, $T_{2\rho}$ and $\Delta\omega_0$ at different FSLs. Spin lock imaging on a phantom ($\text{NiCl}_2 \cdot 6\text{H}_2\text{O}$) and rat livers was performed on a 3T Philips Achieva scanner using a 3D balanced FFE sequence ($\text{TR}/\text{TE} = 5.0/2.5\text{ms}$, $\text{FA} = 30^\circ$, pixel size $= 0.35\text{mm}$, thickness $= 2\text{mm}$) with different FSLs. The delay time after acquisition was set as 4000ms to restore the equilibrium magnetization prior to the next $T_{1\rho}$ preparation.

Results: The magnetization M_z as a function of $T_{1\rho}$, $T_{2\rho}$, TSL and $\Delta\omega_0$ at different FSLs is shown in Fig. 2. M_z shows an attenuated oscillating decay instead of a mono-exponential decay as described by the conventional model. With $\text{FSL} \gg \Delta\omega_0$, the model can be simplified as the conventional

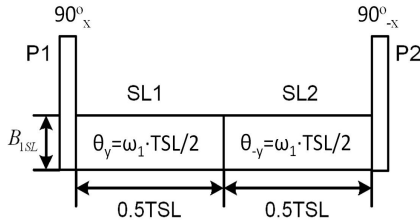


Fig.1. The pulse structure of a SL rotary echo

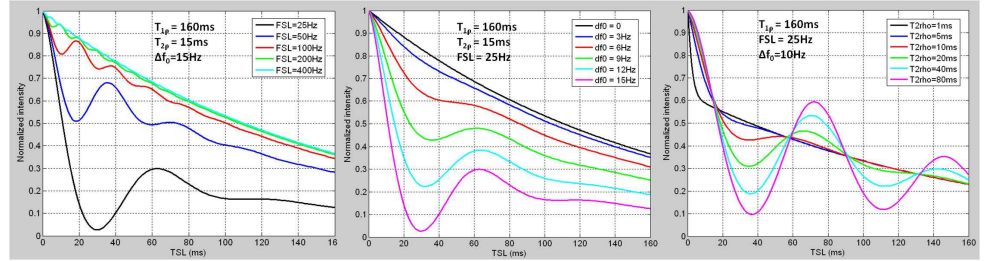


Fig.2. Simulation of longitudinal magnetization as a function of $T_{1\rho}$, $T_{2\rho}$ and $\Delta\omega_0$ at different FSLs

model of mono-exponential decay with TSL. It is seen in Fig.2 that FSL determines the oscillating frequency, $\Delta\omega_0$ determines oscillating amplitude and $T_{2\rho}$ determines oscillating decay rate. $T_{1\rho}$ magnetization decay curves (solid lines) and the fitting curves (dash lines) based on Eq. 3 in phantom and rat liver at FSLs are shown in Fig. 3. Excellent goodness of fit with high coefficient of determination (R^2) over 0.92 was achieved by using the general $T_{1\rho}$ relaxation model for all FSLs except that at 25Hz.

Discussion: As indicated by the general model, the conventional mono-exponential decay model cannot be used for $T_{1\rho}$ mapping at low FSLs because $T_{2\rho}$ and $\Delta\omega_0$ have significant influence on $T_{1\rho}$ weighting. The proposed general is helpful for $T_{1\rho}$ mapping particularly at low FSLs, benefiting patients with much lower RF energy deposit and lower SAR. Another advantage of this general model is that it has potential for simultaneous multi-parameter mapping of $T_{2\rho}$ and off-resonance additional to the normal $T_{1\rho}$ mapping.

Acknowledgement: This work is partially supported by HK GRC grant SEG_CUHK02.

References: [1] Witschey WR et al, JMR 186:75-85(2007); [2] Charagundla SR et al, JMR, 162:113-21(2003);

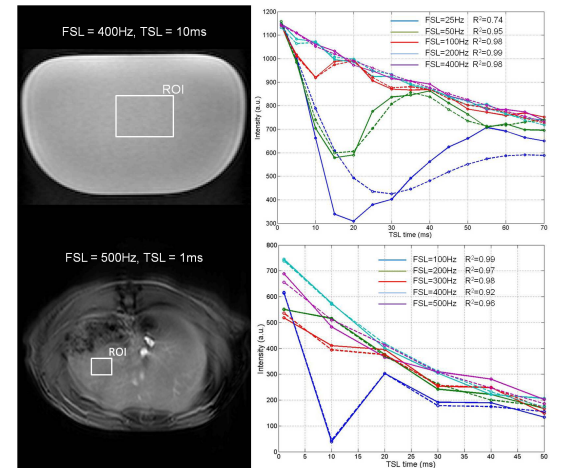


Fig.3. Experimental verification of $T_{1\rho}$ relaxation at different FSLs